

## Evolutionary dynamics of spatial games

Kristian Lindgren<sup>a</sup>, Mats G. Nordahl<sup>b</sup>

<sup>a</sup>*Institute of Physical Resource Theory, Chalmers University of Technology and Göteborg University, S-412 96 Göteborg, Sweden*

<sup>b</sup>*Santa Fe Institute, 1660 Old Pecos Trail, Suite A, Santa Fe, New Mexico 87501, USA*

---

### Abstract

A lattice model of coevolution of strategies for two-person  $2 \times 2$  matrix games is introduced. The model allows evolution in an unbounded space of strategies. In particular we explore the region of parameter space corresponding to the Prisoner's dilemma, and classify the types of dynamical and evolutionary behavior that appear. For certain restricted strategy spaces we explore the complete space of lattice games.

---

### 1. Introduction

One approach to the modeling of coevolutionary systems is to base the interactions between individuals on game theory. In this article, we study the evolutionary dynamics of games in a world with spatial extent, where each individual interacts only with those in a neighborhood around it. In particular we investigate the Prisoner's dilemma, a game which provides a simple framework for studying the evolution of cooperation (see, e.g., [1]).

The spatial extension of the real world is likely to affect evolutionary processes in a number of ways. Mayr [2,3] has argued that the most significant mechanism of speciation is the so-called peripatric speciation, where a small founder population capable of rapid evolution is separated off beyond the periphery of the range of a species, e.g., on an island. Similar ideas can also be found in the original paper on punctuated equilibria by Eldredge and Gould [4].

In this case, the heterogeneity of the physical

world is important; geographical barriers of various kinds allow enough isolation for different evolutionary paths to be explored in different regions. But spatial effects could be important for evolutionary processes even in a homogeneous environment, since the dynamics of the system could give rise to spatial structure.

Spatial effects could for example be of importance to prebiotic evolution—Boerlijst and Hogeweg [5,6] studied a cellular automaton model of the hyper-cycle model of Eigen and Schuster [7], and found spiral wave dynamics which increased the stability against parasites.

Spatial dynamics could also be relevant to the stability of ecological systems, and in that way influence evolutionary processes; as an example, a locally unstable system may persist with essentially constant global population levels through space-time chaos (e.g., [8]).

In this article, we study a simple spatial model where each lattice site contains a single strategy. In each time step every individual plays a game (in most cases the infinitely iterated noisy Prison-

er's dilemma) with its neighbors, and the strategy with the highest score in the neighborhood of a site is allowed to reproduce there. In this way we obtain a model that is essentially a cellular automaton. One can view this either as a model of more or less immobile individuals that each occupy a certain spatial site, or as a simple coarse-grained model of a spatially varying population, where the lattice is divided into regions, and only the most common species in each region is taken into account.

The introduction of spatial degrees of freedom has important consequences for the evolution of cooperation. The spatial dynamics gives rise to new mechanisms for coexistence of cooperative and less cooperative strategies, e.g., through space-time chaos, spiral waves, or in frozen states with stable domain boundaries. The spatial model also allows the evolution of communities with a high degree of diversity.

The rest of this article is organized as follows: In Section 2, the model is presented in detail. In Section 3 the evolutionary dynamics is studied for a particular choice of the pay-off matrix. Sections 4 and 5 explore the rule spaces of spatial games where only memoryless strategies or strategies of very limited memory are allowed. Section 6 gives further details of the evolutionary dynamics in the unbounded strategy space. Section 7 contains a discussion.

## 2. The model

The game we use in most instances is the Prisoner's dilemma, a two-person non-zero-sum game that provides a simple framework for studying the evolution of cooperation – see in particular the pioneering work by Axelrod (e.g., [1]). We consider an infinitely repeated game, where in every round each player has a choice between the two moves C (for cooperate), and D (for defect), and the pay-off matrix  $M$  has the following form:

$$\begin{array}{cc} & \text{Player 2} \\ & \begin{array}{cc} \text{C} & \text{D} \end{array} \\ \text{Player 1} & \begin{array}{cc} \text{C} & \begin{pmatrix} (R, R) & (S, T) \\ (T, S) & (P, P) \end{pmatrix} \\ \text{D} & \end{array} \end{array}$$

where  $T > R > P > S$  and  $2R > T + S$ . These constraints imply that in a single game it is rational for both players to defect, but also that it would be to the mutual advantage of the players to establish cooperation in the long run. In the model, the moves of the players are influenced by noise, so that in each round an intended move is replaced by its opposite with probability  $p_{\text{err}}$ . Sometimes we also consider other symmetric  $2 \times 2$  games.

In the spatial model studied in this article, each site of a regular lattice contains a single individual that plays a certain strategy in the game. An individual at a lattice site only interacts with its neighbors in a neighborhood  $N_1$  of the site. In this article we restrict ourselves to the case of the four nearest neighbors on a 2D square lattice (see Fig. 1).

The dynamics of the model essentially works as follows (a detailed description is given below): playing the game against all neighbors in  $N_1$  gives each individual a total score. All individuals live for a single generation and reproduce simultaneously. The individual with the highest score in a neighborhood  $N_2$  of a certain site gets to reproduce at that site. In the reproduction step mutations may occur.

In an earlier work [9], another model of coevolution of strategies for the Prisoner's dilemma was studied (see also [10] for related work, where the result of the game determined

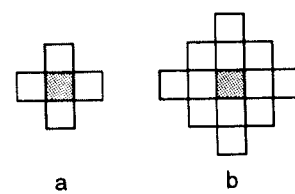


Fig. 1. (a) The neighborhood against which the game is played. (b) The neighborhood affecting the central site at time  $t + 1$ .

the distribution of resources). The population dynamics of that model was based on (discretized) ordinary differential equations (see eq. (1) below), and assumed that in each generation each individual in the population played against all others. In the spatial model, the details of the genetic representation and mutations are identical to those of Ref. [9]. In this way, the model studied in [9] could be viewed as a mean-field approximation to the present model.

The genomes in the model represent strategies in the game. A strategy is a rule for determining the next move of a player given the history  $h = ((x_0, y_0), \dots, (x_t, y_t))$  of the game. The pair  $(x_t, y_t)$  consists of the moves of the player and the opponent, respectively, at time  $t$ . We only consider deterministic strategies of finite memory  $m \geq 0$ . For  $m$  even, the strategy depends on the last  $m/2$  moves of both players; for  $m$  odd on the last  $[(m+1)/2]$  moves of the opponent and the last  $[(m-1)/2]$  moves of the player herself.

If we let 1 denote the action C, and 0 the action D, a strategy of memory  $m$  can be represented as a binary string  $s$  of length  $2^m$ , see Fig. 2. The symbol at position  $i =$

$(b_1, b_2, \dots, b_m)_2$  in  $s$  represents the action when the  $m$  last moves are given by  $\bar{h} = ((b_1, b_2), \dots, (b_{m-1}, b_m))$  for  $m$  even, while for  $m$  odd, the history taken into account is  $\bar{h} = (b_1, (b_2, b_3), \dots, (b_{m-1}, b_m))$ , so that of the actions at time  $t - [(m+1)/2]$ , only the move of the opponent can affect the strategy.

In the reproduction of a strategy, three types of mutations may occur: point mutations, gene duplications, and split mutations. Point mutations flip single bits in the genome with frequency  $p_{\text{mut}}$ . The gene duplication operator increases the memory of a strategy from  $m$  to  $m + 1$  (with frequency  $p_{\text{dupl}}$ ) while leaving the actual strategy unchanged. This corresponds to duplicating the genome:  $1011 \rightarrow 10111011$ , for example.

Gene duplication is a neutral mutation, which increases the size of the evolutionary search space without immediately affecting the phenotype. Additional point mutations can then give rise to new strategies without shorter memory equivalents. In this way, we may consider evolution in an unbounded space of strategies (though in a computer implementation the maximal memory allowed is of course bounded).

Finally, the split mutation splits a genome into two parts of equal size with frequency  $p_{\text{split}}$ ; one of these is chosen at random and kept in the population.

Each lattice site is occupied by a single strategy; empty lattice sites are not allowed. All lattice sites are updated simultaneously in the following manner: first the score of a site  $(i, j)$  is calculated as the sum of the average scores obtained when the strategy  $s(i, j)$  at the site plays the infinitely iterated game against the strategies in the neighborhood  $N_1$  (the four nearest neighbors in the case studied here).

The score of a site is then compared to the scores in a neighborhood  $N_2$  (taken as the von Neumann neighborhood consisting of the site itself and its four nearest neighbors), and the highest scoring strategy in  $N_2$  is adopted at  $(i, j)$  at the next time step. Note that the neigh-

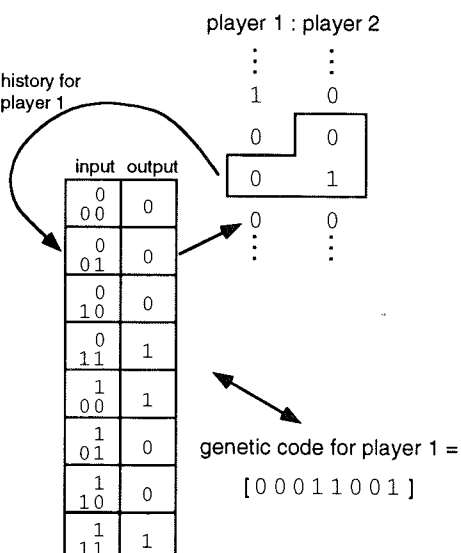


**Fig. 2.** The representation of strategies as binary strings is illustrated for the memory 3 strategy 00011001

borhood  $N_2$  includes the site itself. Ties are broken by adding a very small amount of random noise to the scores. Since the scores of the nearest neighbors in turn depend on the strategies of their neighbors, the strategy at a certain site is actually updated depending on the strategies in a neighborhood of radius 2 (see Fig. 1b). This means that if we were to restrict ourselves to a finite set of strategies, the model would be a cellular automaton.

Similar CA models (but with a fixed set of strategies and without evolution) were introduced by Axelrod in [1]; in [11,12] the dynamics of the memoryless strategies C and D on a lattice was studied in more detail. For a different approach to a spatial Prisoner's dilemma based on an  $n$ -person game where strategies depend on all actions in the neighborhood of a site, see Refs. [13,14].

The interaction between two individuals is *a priori* described by five parameters:  $R, S, T, P$ , and the error rate  $p_{\text{err}}$ . However, the dynamics described above is invariant under affine transformations of the pay-off matrix of the form  $M \leftarrow aM + bM_1$ , where  $M_1 = \begin{pmatrix} 1 & 1 \\ 1 & 1 \end{pmatrix}$  and  $a > 0$ . If  $R - S > 0$ , this means that we can choose a normal form for the pay-off matrix where  $(R', S', T', P') = (1, 0, p, q)$ , with  $1 < p < 2$  and  $0 < q < 1$  for the Prisoner's dilemma. If  $R - S < 0$ , we can instead find an equivalent game of the form  $(-1, 0, p, q)$ .

This leaves three parameters; in the simulations below we study the effects of varying the error rate with a fixed pay-off matrix given by  $(R, S, T, P) = (1, 0, \frac{5}{3}, \frac{1}{3})$  (equivalent to the commonly used  $(3, 0, 5, 1)$ ), and of varying the pay-off matrix with the error rate fixed at  $p_{\text{err}} = 0.01$ .

The results from the model will sometimes be compared to the results of the mean-field model of [9], where everyone plays against everyone. In this model, each strategy  $i$  has a real-valued population size  $x_i$ . The population densities evolve in time according to

$$\Delta x_i = \alpha x_i \left( \sum_j g_{ij} x_j - \Phi \right), \quad (1)$$

where the term (identical to the average score of the population)

$$\Phi = \sum_{i,j} g_{ij} x_i x_j \quad (2)$$

ensures that the total population stays constant. The interaction coefficient  $g_{ij}$  is the score obtained when strategy  $i$  plays strategy  $j$ . At each time step, mutations act in the way described above. In this way new species can be introduced. Species are removed from the system if their population falls below a threshold value.

### 3. Evolutionary dynamics—an example

A first example of the behavior of the model is obtained by letting  $(R, S, T, P) = (1, 0, \frac{5}{3}, \frac{1}{3})$ ,  $p_{\text{err}} = 0.01$ ,  $p_{\text{mut}} = 0.002$ , and  $p_{\text{dupl}} = p_{\text{split}} = 0.001$ . In the initial state each site is randomly assigned one of the four memory 1 strategies with equal probability. The results of a typical simulation are shown in Figs. 3 and 4. The lattice size in this case is  $128 \times 128$ .

After some initial oscillations, a state dominated by 00 (All D), 11 (All C), and 01 (Tit-for-Tat) with fairly constant densities is reached. A snapshot of the spatial structure during this period of stasis is shown in Fig. 4a. The always cooperating strategy 11 forms stable islands in a sea of 00 defectors; 01, alias Tit-for-Tat, can invade a homogenous configuration of All D, but

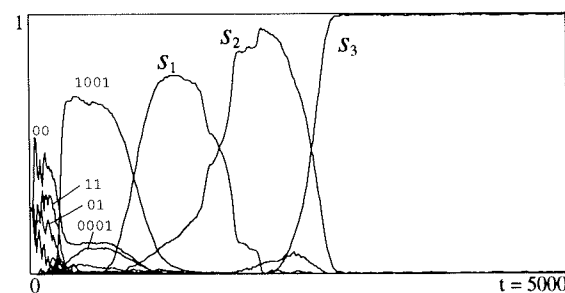


Fig. 3. Population densities as function of time for the parameter values  $(p, q) = (\frac{5}{3}, \frac{1}{3})$ ,  $p_{\text{err}} = 0.01$ . The first 5000 generations of the simulation are shown.

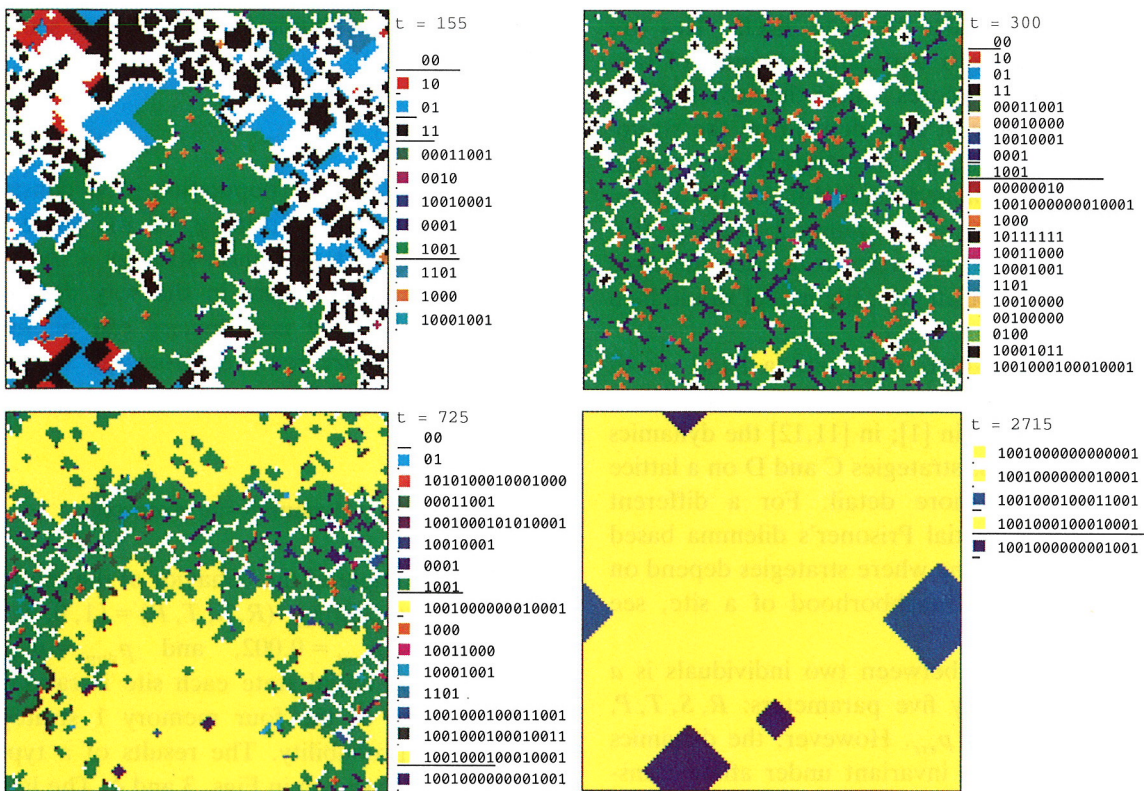


Fig. 4. Examples of lattice configurations during the simulation of Fig. 3. (a)  $t = 155$ : frozen domains of 00 and 11; waves of 01. (b)  $t = 300$ : 1001 dominates, 00 and 0001 at low levels. (c)  $t = 725$ : the previous state is invaded by  $s_1 = 1001000100010001$ . (d)  $t = 2715$ : domain of  $s_2 = 1001000100011001$  growing in a sea of  $s_1$ .

is in turn invaded by All C. Mutations from 00 to 01 generate spreading waves of activity. In this way, Tit-for-Tat is maintained at a fairly high density. Some 10 mutants also appear. If mutations are turned off, the system will freeze with only a few stable Tit-for-Tat domains remaining.

This period of stasis is interrupted by the appearance of the memory 2 strategy 1001, which spreads rapidly and takes over almost the entire lattice. This strategy is capable of correcting single errors and returning to a pattern of cooperation when playing against itself [9]; an accidental defection  $D^*$  would result in the sequence  $(\dots, CC, CD^*, DD, CC, CC, \dots)$ , where a single round of mutual defection signals a return to cooperation.

Fig. 4b shows a typical state during this second period of stasis. We can see that 00 and 0001 are

able to coexist with 1001 at low densities. These strategies tend to form a network of mostly diagonal lines where each mutant plays against two 1001 individuals, but many other stable shapes are also possible. Some other mutants (such as 1000) may also enter in small quantities. These can be strategies which exploit 1001, but less efficiently than 00 or 0001, and at the same time do not play well against themselves. This means that a single mutant site may be stable, but unable to grow. The appearance of another mutant of the same kind next to it would lower the score of both and cause their extinction.

No memory 3 strategy appears to be able to invade this state, but at least two memory 4 strategies can do so. In the simulation, the first memory 4 strategy to enter is  $s_1 = 1001000100010001$  (one point mutation away

from the quadruplicate of 0001, which is present in small numbers), which takes over most of the lattice, except for small stable islands of 1001. Fig. 4c shows the lattice during the invasion process. A smaller domain of another memory 4 strategy,  $s_2 = 1001000100011001$ , is already present. The strategy  $s_2$  can invade the state dominated by  $s_1$ , and enters slowly at first, then rapidly after it reaches a majority of the population. This is a geometrical effect: small diagonally oriented rectangular domains of  $s_2$  in a background of  $s_1$  are stable in the absence of mutations; mutations along the edges trigger growth events which extend an entire edge by a site. Once  $s_2$  reaches a significant size, a phase of much faster growth is entered, since domains of  $s_1$  in a background of  $s_2$  will be attacked at convex corners and shrink away rapidly. Fig. 4d shows a growing domain of  $s_2$  in a sea of  $s_1$ , together with two smaller domains of the closely related strategy 100100000001001, which is later eliminated by  $s_2$ . Notice the steps along the edges that propagate to extend the side by one site.

The strategy  $s_2$  is then replaced by  $s_3 = 1001000000010011001000100011001$ , a memory 5 strategy which also forms a homogenous state. This strategy appears to be very stable against memory 5 mutants, at least on a time scale of  $10^5$  generations. We have not yet explored longer memory.

All three strategies  $s_1$  to  $s_3$  share the same mechanism for correcting for accidental defections – both players defect twice after a single defection and then return to cooperation. This pattern restores cooperation, but at the same time does not allow other strategies to exploit the cooperative behavior.

Some less common evolutionary paths avoid this homogenous memory 5 state. This can happen if a strategy  $t_1 = 1001000000001111$  (or some of its closer mutants) manages to establish itself earlier in the evolution. This is often preceded by a period of unstable dynamics where other memory 4 strategies replace  $s_1$  and

$s_2$ . When two  $t_1$  strategies play against each other, an accidental defection  $D^*$  is answered first by mutual cooperation, then by mutual defection, and after that they return to cooperation, i.e., ( $\dots, CC, CD^*, CC, DD, CC, CC, \dots$ ). This means that  $t_1$  behaves like 1001 that dominated earlier in the evolution, but with an extra round of cooperation inserted before the response to a defection. The advantage of this pattern is that accidental defections do not reduce the score as much as the error correcting mechanism of, e.g.,  $s_2$  or  $s_3$ . It also means that  $t_1$  is more resistant than 1001 to exploitation by the simple All D strategy.

A simulation where  $t_1$  enters is shown in Fig. 5. That simulation actually ends (see Fig. 6) with coexisting almost frozen regions of  $s_3$  and two memory 5 variations of  $t_1$ .

We can compare these results to what happens in the model described by Eq. (1), where everyone plays against everyone. Fig. 7 (copied from [9]) shows a typical simulation of this model, with a pay-off matrix given by  $(R, S, T, P) = (3, 0, 5, 1)$ , and starting from an initial state where all four memory 1 strategies have equal populations.

At memory 1, the behavior of the spatial model is entirely different from the mean-field model, where a stable state with coexistence of 01 and 10 is found. The strategy 1001 which dominates at memory 2 shows up in the mean-field model as well, but there it is more efficiently exploited by 0001, which has a slight advantage over 1001 and dominates at memory 2. In the lattice model, the exploitation is less efficient due to the geometry, which allows cooperative strategies to cluster, and limits non-cooperative strategies to exploiting their nearest neighbors. In this case the cooperative strategy 1001 has an advantage.

At memory 3, the symbiotic pair of strategies 10010001 and 00011001 seen in Fig. 7 usually dominates in the mean-field model (see [9] for details). No analogue of this symbiotic pair appears to exist in the spatial model.

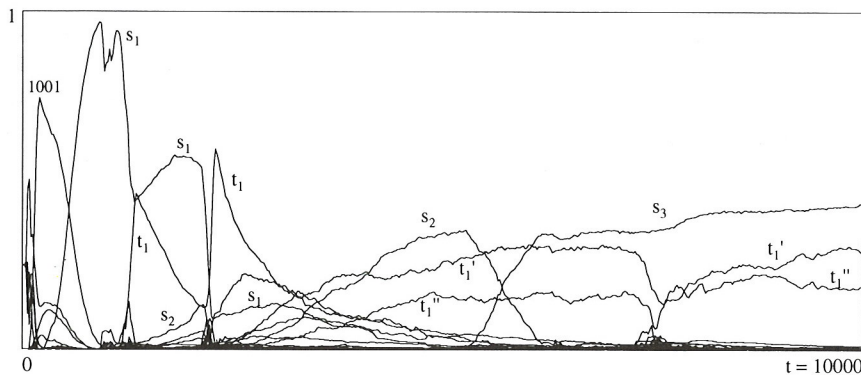


Fig. 5. Another simulation for the same parameter values as Fig. 3, showing an alternative evolutionary path. The first 10000 generations of the simulation are shown.

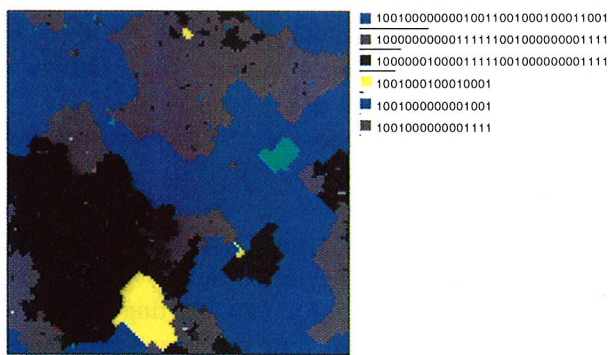


Fig. 6. Lattice configuration from the end of the simulation of Fig. 5 (at  $t = 8000$ ), showing coexistence between strategies of types  $s_3$  and  $t_1$ .

The memory 4 strategies  $s_1$  and  $s_2$  that appear on the lattice both belong to a group of strategies often encountered as a very stable final state of

the mean-field model (several of which are evolutionarily stable against single mutants). In Fig. 7 the strategy  $s_1 = 100100010001001$  is the first to enter; mutations then cause a group of similar, nearly degenerate strategies to coexist as a quasispecies at large times.

In the lattice model a single strategy  $s_2$  among these often takes over the entire population even in the presence of mutations. The higher degree of discrimination is due to the fact that the highest scoring strategy in the neighborhood  $N_2$  always is reproduced, instead of making a stochastic choice according to the scores. In this way only the relative ordering of the scores matter, not the score differences. This is also why a slightly refined memory 5 strategy is able to completely eliminate  $s_2$ .

In the spatial model we also see the appearance of strategies of type  $t_1$ . By forming do-

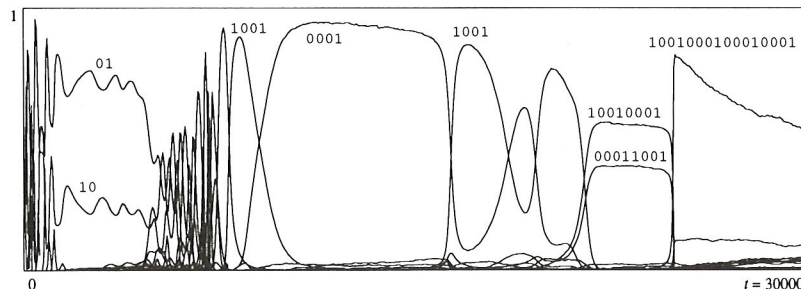


Fig. 7. Population densities as function of time for the model described by Eq. (1), where all pairwise interactions between strategies are included.

mains, these strategies can coexist with  $s_2$  and  $s_3$  – a phenomenon that has not been observed in the mean field model.

#### 4. Cooperators and defectors on a lattice

To analyze the dynamics of the system in more detail, let us first consider a community consisting only of cooperators and defectors, i.e., of the two memoryless strategies C and D. In this case, the iterated game between two strategies is equivalent to a sequence of independent single games. Errors by the players are somewhat less significant in this simple case, since a change in the error probability only corresponds to a rescaling of the pay-off matrix.

We also temporarily disregard the evolutionary dynamics, i.e., we let  $p_{\text{mut}} = p_{\text{dupl}} = 0$ . If we introduce dynamics in the way described above, our lattice system then simply becomes a 2-state radius 2 deterministic cellular automaton.

Consider a constant size population of memory 0 strategies where everyone plays the Prisoner's dilemma against everyone. Defectors will then eventually take over completely, since in that case defection is a dominant strategy for all values of  $(p, q)$  and  $p_{\text{err}}$ . In the spatial system, the situation is considerably more complicated. In particular, the spatio-temporal dynamics may give rise to the coexistence of cooperators and defectors. This could for example happen if the system goes to a fixed point containing stable domains of cooperators, or through space-time chaos (see also Nowak and May [11,12], where a subspace of the rule space of this section was studied).

If we fix the error probability to  $p_{\text{err}} = 0.01$  and vary the pay-off matrix inside the Prisoner's dilemma region  $1 < p < 2$  and  $0 < q < 1$ , we numerically find 5 regions of qualitatively different asymptotic behavior for the spatial memory 0 system, see Figs. 8 and 9:

(1) Homogenous state of defectors.

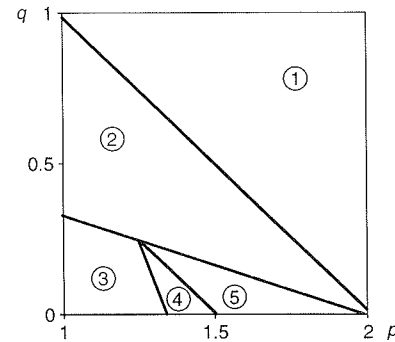


Fig. 8. Phase diagram for asymptotic behavior of memory 0 strategies when the pay-off matrix is varied ( $p_{\text{err}} = 0.01$ ,  $p_{\text{mut}} = 0$ ).

- (2) Stable small domains of cooperators in a background of defectors, see Fig. 9a.
- (3) Stable percolation network of defectors in a background of cooperators, see Fig. 9b.
- (4) Space-time chaos—a fixed configuration of the system is shown in Fig. 9c.
- (5) Cooperators can form organized spatial

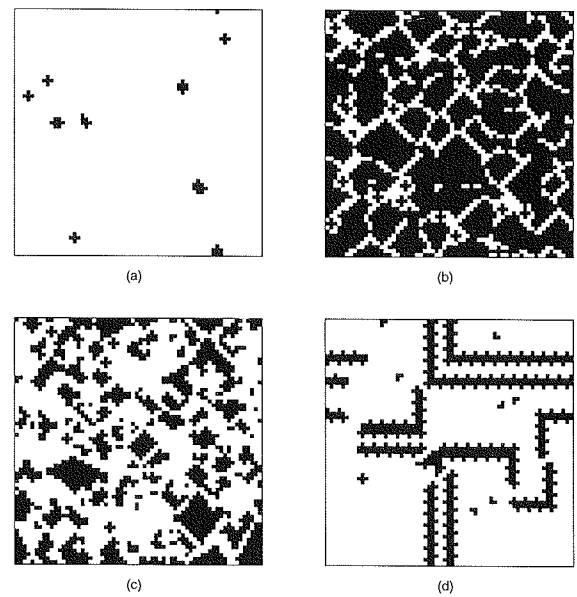


Fig. 9. Typical configurations from simulations with parameters from (a) region 2 of the memory 0 phase diagram,  $(p, q) = (\frac{5}{3}, \frac{1}{3})$ ; (b) region 3,  $(p, q) = (1.2, 0.2)$ ; (c) region 4,  $(p, q) = (1.4, 0.05)$ ; (d) region 5,  $(p, q) = (1.6, 0.05)$ .

structures of the form shown in Fig. 9d. These form by linear growth from small seeds, and eventually reach a steady state. The smaller objects in Fig. 9d oscillate with period 2 or 4.

The structure of this phase diagram can to a large extent be calculated analytically. For simplicity, we begin by considering the case without mistakes, i.e.,  $p_{\text{err}} = 0$ . In that case, a cooperator can receive a total score of 0, 1, 2, 3 or 4 (identical to the number of cooperating nearest neighbors), while a defector can receive a score of  $4p$ ,  $3p + q$ ,  $2p + 2p$ ,  $p + 3q$  or  $4q$  (or  $pn + q(4 - n)$ , where  $n$  is the number of cooperating nearest neighbors). This means that when  $p$  and  $q$  are varied, the actual cellular automaton rule can only change when we cross one of the lines  $mp + (4 - m)q = n$ , where  $m, n \in \{0, 1, 2, 3, 4\}$ .

This gives us a partition of the  $(p, q)$ -plane into a number of regions, where each region corresponds to a single CA rule. Different regions in this partition may still contain the same CA rule – as an example, on one side of the line  $4q = 4$  the score of the neighborhood  $\begin{array}{|c|c|c|} \hline 0 & 0 & 0 \\ \hline 0 & 1 & 0 \\ \hline 0 & 0 & 0 \\ \hline \end{array}$  is higher than that of  $\begin{array}{|c|c|c|} \hline 1 & 1 & 1 \\ \hline 1 & 0 & 1 \\ \hline 1 & 1 & 1 \\ \hline \end{array}$ , on the other side the order is reversed. But since no radius 2 neighborhood can simultaneously contain these two configurations, this transition is irrelevant for the dynamics.

An exhaustive analysis of these transitions [15] results in the diagram shown in Fig. 10, where the  $(p, q)$ -plane is divided into 157 regions, corresponding to distinct cellular automaton rules. The Prisoner's dilemma region is marked in the figure. The transitions between different CA rules do not follow the boundary of this region – in other words, in this case the classification of elementary spatial games bears little relation to the classification of  $2 \times 2$  games in terms of their properties when played only once [16]. As an example, the partition diagram shows that regions 4 and 5 of Fig. 8 extend well outside the Prisoner's dilemma region into the Chicken region, where  $T > R > S > P$ .

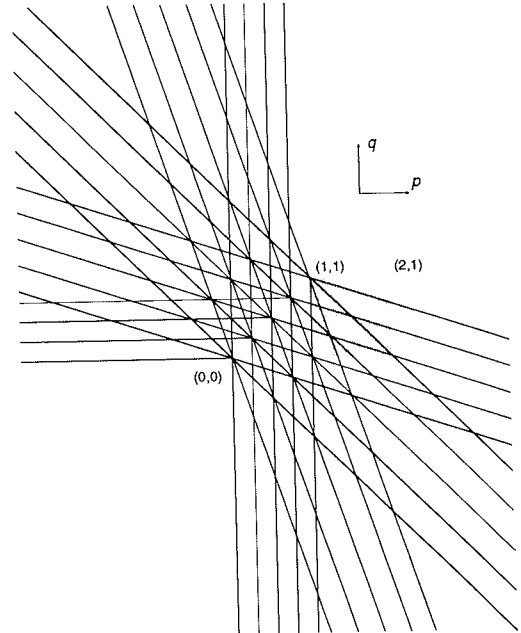


Fig. 10. Diagram showing the complete partition of the  $(p, q)$ -plane into regions containing distinct CA rules for  $p_{\text{err}} = 0$ . The Prisoner's dilemma region ( $1 < p < 2$  and  $0 < q < 1$ ) is shaded in the figure.

This analysis gives us the complete set of cellular automaton rules for  $p_{\text{err}} = 0$ . For memory 0 strategies, there is a simple transformation from this case to arbitrary error probabilities. If the pay-off matrix is given by the parameters  $(p, q)$ , and the error rate is  $\epsilon$ , the game is equivalent to an error-free game with a pay-off matrix given by

$$\begin{aligned} (R', S', T', P') = & ((1 - \epsilon)^2 + \epsilon(1 - \epsilon)p + \epsilon^2 q, \\ & \epsilon(1 - \epsilon)(1 + q) + \epsilon^2 p, \\ & (1 - \epsilon)^2 p + \epsilon(1 - \epsilon)(1 + q), \\ & (1 - \epsilon)^2 q + \epsilon(1 - \epsilon)p + \epsilon^2), \end{aligned} \quad (3)$$

which, if  $R' > S'$ , can be transformed to the normal form

$$(p', q') = \left( \frac{(1 - 2\epsilon - 2\epsilon^2)p}{(1 - \epsilon)^2 + \epsilon(1 - \epsilon)(p - 1 - q) + \epsilon^2(q - p)}, \frac{(1 - \epsilon)^2q + \epsilon(1 - \epsilon)p + \epsilon^2}{(1 - \epsilon)^2 + \epsilon(1 - \epsilon)(p - 1 - q) + \epsilon^2(q - p)} \right). \quad (4)$$

In the same way as above we then consider the partition of the  $(p', q')$ -plane given by  $mp' + (4 - m)q' = n$  where  $m, n \in \{0, 1, 2, 3, 4\}$ , or  $(m(1 - 2\epsilon - 2\epsilon^2)p + (4 - m)\epsilon(1 - \epsilon)p + (4 - m)(1 - \epsilon)^2q + (4 - m)\epsilon^2 = n$ , which shows how the phase diagram for non-zero noise levels is obtained from that for  $p_{\text{err}} = 0$  by an affine transformation. Further details (e.g., the case  $R' < S'$ , and further discussion of games other than the Prisoner's dilemma) will be given in [15].

Note that the experimental phase diagram in Fig. 8 does not distinguish between all the CA rules in the partition of Fig. 10 (there are for example 11 distinct CA rules in the Prisoner's dilemma region). The reason for this is that even though two regions contain different CA rules, this might only show up, e.g., in minor differences in the transient behavior. These do not affect the "macroscopic" phase diagram of Fig. 8, which is based on statistical properties of the long-term behavior.

An example of this is given by considering the line  $p + 3q = 4$  where it passes through region 1 of Fig. 8 (where defectors dominate asymptotically). For the CA rule with  $p + 3q > 4$  defectors dominate unconditionally, i.e., any site with a D in the neighborhood  $N_2$  at time  $t$  turns into a D at  $t + 1$ . When  $3 < p + 3q < 4$ , a defecting site still remains a defector forever, but now horizontal and vertical boundaries are stable. A domain of C can however still be attacked at corners and diagonal boundaries, and the only fixed point configurations are homogenous states of D.

In general, the asymptotic behavior (e.g., the invariant probability measure) of a 2d CA rule can only be calculated approximatively, which means that one has to rely on numerical experiments to classify the rules of Fig. 10 into larger regions. In the next section, we shall consider the dynamics of memory 1 strategies. In that case, the number of rules in the corresponding

microscopic phase diagram is many orders of magnitude larger, which makes an analytic treatment impractical and a coarse-grained description even more relevant.

## 5. Dynamics of memory 1 strategies

If we also allow memory 1 strategies, i.e., we consider the dynamics in the space consisting of the four strategies 00 (always defect), 01 (Tit-for-Tat), 10 (Anti-Tit-for-Tat, or ATfT), and 11 (always cooperate), several new dynamic phenomena appear. Even though our main interest is the evolutionary dynamics in the unbounded strategy space, the dynamics in this subspace of strategies is of some relevance, since an initial period of stasis dominated by memory 1 strategies almost always is observed in the simulations.

Let us first consider the case where the pay-off matrix is fixed to  $(R, S, T, P) = (1, 0, \frac{5}{3}, \frac{1}{3})$  and the error rate is varied between 0 and 0.5. We study the long-term behavior of a system where initially all four memory 1 strategies are present at equal density, and the system evolves according to the dynamics described above, with a non-zero point mutation rate ( $p_{\text{mut}} = 0.002$ ), but no gene duplications ( $p_{\text{dupl}} = 0$ ).

We then find the following behavior:

- $0.0 < p_{\text{err}} \leq 0.148$ . Frozen state of 00 and 11; waves of 01 are maintained by mutations.
- $0.148 \leq p_{\text{err}} \leq 0.226$ . Space-time chaos involving 01 and 11, see Fig. 11.
- $0.226 \leq p_{\text{err}} \leq 0.244$ . Transition region with slowly shifting domains of 11 in a background of 01, together with frozen 00/11 domains.
- $0.244 \leq p_{\text{err}} \leq 0.269$ . Single 00 sites in a 01 background.
- $0.269 \leq p_{\text{err}} \leq 0.341$ . Network of lines of 00 in a background of 01.
- $0.341 \leq p_{\text{err}} \leq 0.419$ . Small islands of 01 in a sea of 00.
- $0.419 \leq p_{\text{err}} < 0.5$ . Small islands of 01 or 10 in a sea of 00.

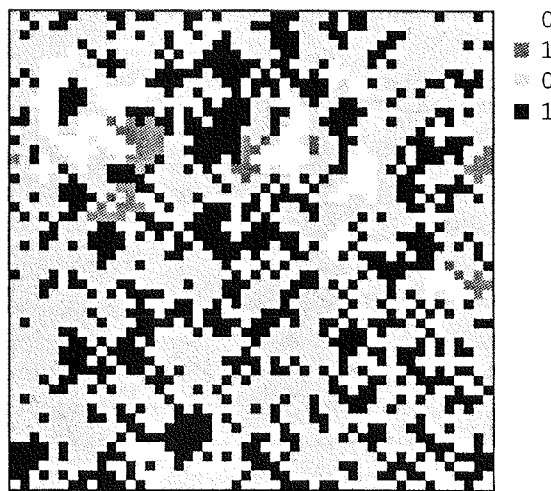


Fig. 11. A configuration from a memory 1 simulation with  $p_{\text{err}} = 0.15$ .

- $p_{\text{err}} = 0.5$ . Completely random play, i.e., all strategies are equivalent. Domains are formed because of the finite neighborhood used in the reproduction step; domain walls move randomly.

In other words, when the error rate is increased from  $p_{\text{err}} = 0$ , we first encounter a frozen phase of All C and All D (and TtT generated by mutations), then a chaotic phase dominated by TtT and All C. For very high error probabilities, we once again find a frozen phase, where first Tit-for-Tat and finally All D dominate as we approach  $p_{\text{err}} = 0.5$ .

Let us now instead fix the error rate to  $p_{\text{err}} = 0.01$ , and let the pay-off matrix be given by  $(R, S, T, P) = (1, 0, p, q)$ , with  $1 \leq p \leq 2$  and  $0 \leq q \leq 1$  for the Prisoner's dilemma. The analytic approach of the previous section is impractical in this case, but we can use a similar argument to obtain an upper bound on the number of CA rules in the  $(p, q)$ -plane for the memory 1 case.

The score of a certain neighbourhood depends on the strategy at the central site and the number of strategies of each kind among its four neighbour, i.e., for the purpose of calculating the score we can represent the neighborhood as  $(c; n_{11}, n_{10}, n_{01})$ , where  $c$  is the strategy of the

central site, and we have  $n_{11}, n_{10}, n_{01} \in \{0, 1, 2, 3, 4\}$  and  $n_{11} + n_{10} + n_{01} \leq 4$ .

For each  $c$ , there are 35 possible assignments of  $n_{11}$ ,  $n_{10}$ , and  $n_{01}$ , or in other words 35 possible total scores for the strategy  $c$  depending on the neighborhood (assuming no degeneracies). Considering all pairwise comparisons of total scores gives a partition of the  $(p, q)$ -plane into regions containing a single CA rule (but still possibly the same CA rule in different regions). The total number of such comparisons is  $6 \times 35^2 = 7350$  (compared to 25 for memory 0), which means that the total number of regions can be at most 27007576, since  $n$  lines can divide the plane into at most  $n(n - 1)/2 + 1$  regions.

If we exclude all comparisons between two neighborhoods that have no strategy in common, and thus cannot be found simultaneously in a radius 2 neighborhood, the number of relevant comparisons is reduced to 6924. The upper bound on the number of distinct CA rules is then 23 967 427. The actual number of memory 1 CA rules is undoubtedly smaller than this bound, but we see no reason why it could not be of a comparable order of magnitude (for memory 0, an analogous argument gives an upper bound of 277 rules; the actual number is 157).

Numerically we can, e.g., measure the asymptotic population densities of various strategies. Figs. 12a–12d show numerical results for the steady state densities of the strategies 00, 01, 10, and 11 in a system where only point mutations are allowed ( $p_{\text{mut}} = 0.002$ ). Each point in these diagrams is based on an average over 5 runs on a  $100 \times 100$  lattice, where densities were time averaged from  $t = 1000$  to  $t = 1500$ .

The phase diagram in Fig. 13 then summarizes the different types of behavior that appear when the pay-off matrix is varied. Eight principal regions of this diagram can be identified:

- (1) Homogenous state of 11.
- (2) Space-time chaos involving 00, 01, and 11 (see Fig. 14a) – closely related to the 00/11 chaos in region 4 of Fig. 8.
- (3) Frozen state of 00 and 11; waves of 01 (see

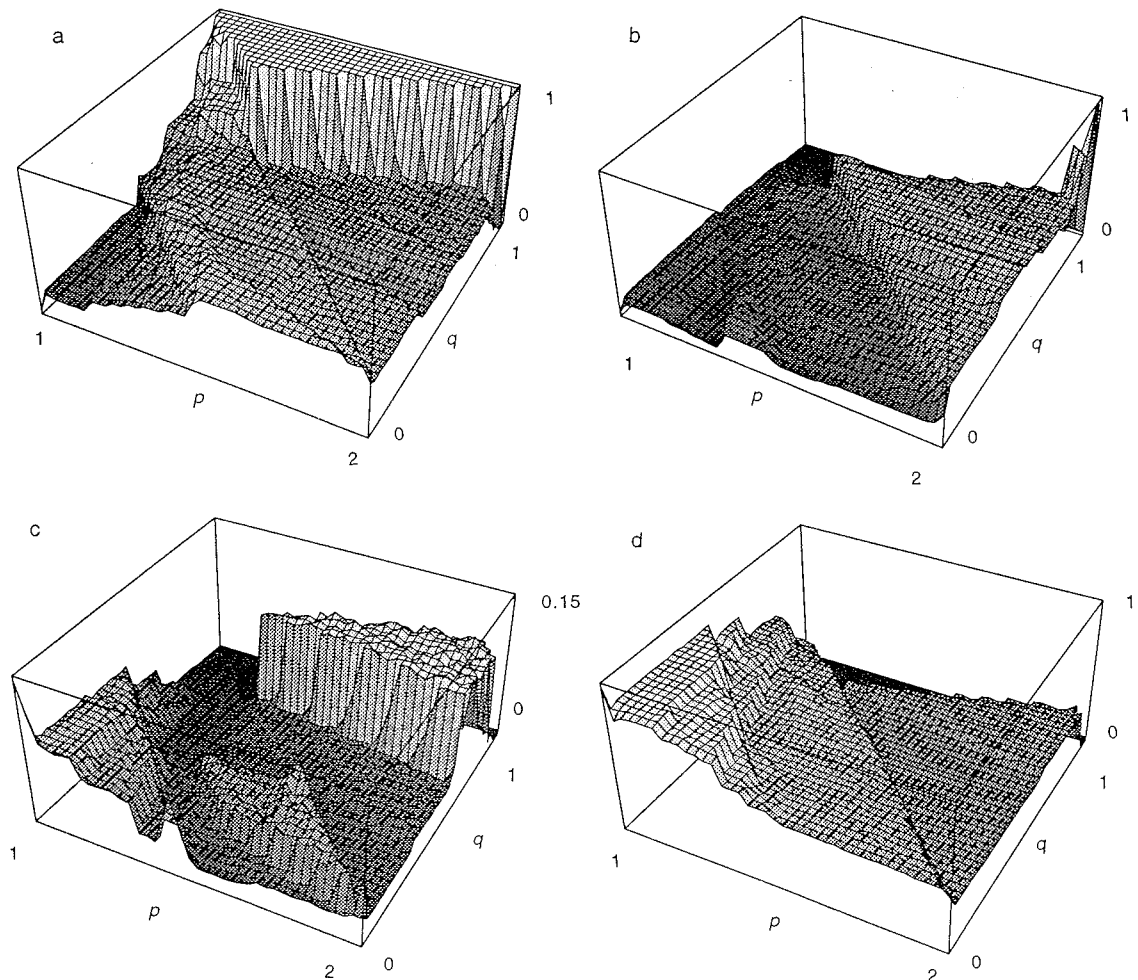


Fig. 12. Invariant densities of memory 1 strategies as function of  $p$  and  $q$  when only point mutations are allowed ( $p_{\text{err}} = 0.01$ ,  $p_{\text{mut}} = 0.002$ ). (a) Density of 00; (b) density of 01; (c) density of 10; (d) density of 11.

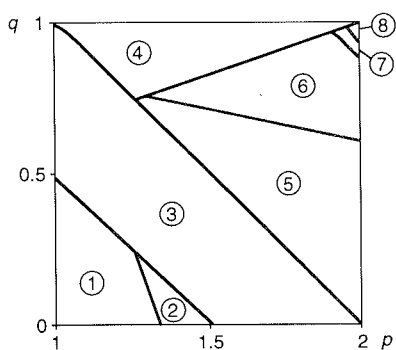


Fig. 13. Phase diagram for memory 1 when the pay-off is varied ( $p_{\text{err}} = 0.01$ ,  $p_{\text{mut}} = 0.002$ ).

Fig. 4a). The point  $(p, q) = (\frac{5}{3}, \frac{1}{3})$  discussed above is located inside this region close to the boundary.

- (4) Homogenous state of 00.
- (5) Spiral waves of 00, 01, and 11 (see Fig. 14b).
- (6) Irregular wave fronts and patches (see Fig. 14c).
- (7) Space-time chaos involving 01 and 11, similar to Fig. 11.
- (8) Homogenous state of 01.

In most of the cases 1–8, additional strategies may be present at low densities because of mutations. Most of the transitions are clearly

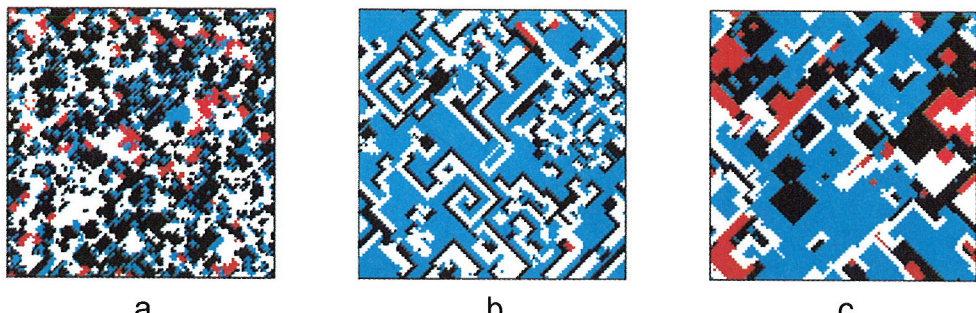


Fig. 14. Examples of typical configurations from simulations with parameters from (a) region 2 of the memory 1 phase diagram,  $(p, q) = (1.4, 0.05)$ ; (b) region 5,  $(p, q) = (1.9, 0.2)$ ; (c) region 6,  $(p, q) = (1.9, 0.8)$ .

indicated in the density plots of Fig. 12. The transitions to the chaotic regions are an exception; in those cases a more appropriate order parameter is the spreading rate of small perturbations [17,18]. We shall explore this further elsewhere [15].

Some of the transitions show up in unexpected ways in the density plot – consider for example the transition between regions 5 and 6. In region 5, spiral wave patterns consisting of 00, 01, and 11 are formed (often rather irregular because of mutations, which tend to break the rather thin spirals into fragments). Mutants of the form 10 are eliminated by the spatiotemporal dynamics, a phenomenon reminiscent of what happens in the spatial hypercycle model [5,6]. In region 6, where wave fronts and patches move in a more irregular way, ATfT mutants are considerably more successful. This can clearly be seen in Fig. 12c which shows the 10 density.

Some of the structure of phase diagram in Fig. 13 depends crucially on the presence of mutations. In particular, on both sides of the boundary between regions 1 and 3 the CA dynamics initially reaches an essentially homogenous state of 11. On the region 3 side, however, this state is not stable towards mutations to 00, and on a longer time scale defectors take over most of the lattice.

Some other phenomena that involve the spatial degrees of freedom in an essential way are also observed for memory 1. We have observed

several different types of gliders (stable propagating structures), in particular close to the border of region 4, where defectors take over completely. Fig. 15 shows some examples. One may note that this occurs at a percolation-like transition between a region where the system goes to a homogenous state and another where activity propagates to infinity, and not at the transition to chaos.

Another phenomenon that also depends on the spatial degrees of freedom is that of a critical size for growth of clusters of cooperative mutants. One example of this occurs close to the transition from region 8 to region 4. There Tit-for-Tat can only expand in a sea of defectors

once small TfT clusters such as are formed.

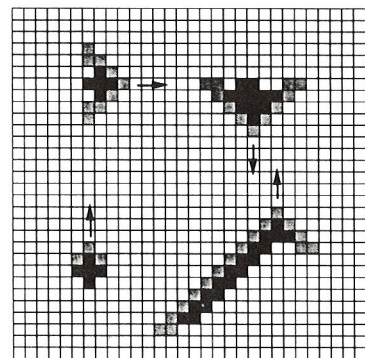


Fig. 15. Some examples of gliders found at  $(p, q) = (1.2, 0.815)$ .

## 6. Evolutionary dynamics

When gene duplications and split mutations are allowed, the evolutionary process takes place in an essentially unbounded space (disregarding implementation limits), where strategies may become arbitrarily complex. When the parameter values are varied, a rich variety of evolutionary and dynamic behavior is found, and a complete discussion would be beyond the scope of this paper. Instead we shall give some examples that illustrate some of the more important types of behavior that are observed.

Some general properties of the system have already been demonstrated in the simulations of Section 3, where  $(p, q) = (\frac{5}{3}, \frac{1}{3})$ . In particular, these simulations showed how it is possible for a single strategy to asymptotically form a spatially homogenous state and resist invasion, and also the possibility of coexistence of a small number of strategies through the formation of stable spatial domains.

A property shared by the spatial model and the mean-field model is that the dynamics often is characterized by stable periods separated by periods of rapid evolutionary change, a behavior reminiscent of punctuated equilibria [4]. In the spatial model, the transitions between periods are often somewhat more gradual, since exponential growth cannot occur because of the finite spreading rate. A fairly high mutation rate was used to speed up the simulations; this also shortens the stable periods.

In the previous sections we have discussed the behavior of the system in the subspaces of memory 0 and memory 1 strategies. This behavior correlates rather well with stable periods in the unbounded system.

We could consider the behavior of memory 2 strategies in the same way. The relation to the unbounded system then becomes somewhat less direct – for some parameters, stable periods may involve strategies of several different memory lengths, and sometimes no memory 2 period of stasis appears at all. Multiple evolutionary paths are also possible for some parameter values.

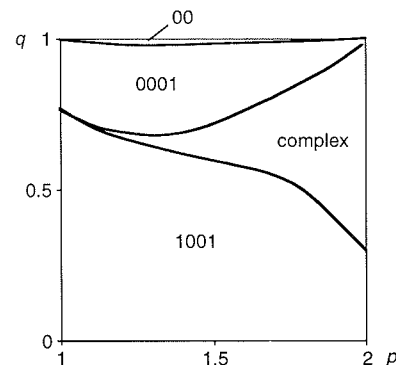


Fig. 16. Approximate classification of memory 2 periods of stasis when the pay-off matrix is varied ( $p_{\text{err}} = 0.01$ ,  $p_{\text{mut}} = 0.002$ ).

Fig. 16 instead shows the typical behavior at memory 2 starting from an initial state consisting of all four memory 1 strategies with equal densities. In the regions marked by 00, 0001, and 1001, we find frozen states dominated by these strategies; the remaining region is characterized by non-trivial spatiotemporal dynamics and complex behavior, e.g., coexistence of strategies of different memory, and patchy frozen states of high diversity.

The asymptotic behavior also varies in different regions of parameter space. An example showing behavior different from that of Section 3 is given by the simulations shown in Figs. 17 and 18, where  $(p, q) = (1.95, 0.95)$ , and  $p_{\text{err}} = 0.01$ . For these parameter values we initially find space-time chaos involving Tit-for-Tat and All C, see Fig. 18a. We then observe evolution towards more complex strategies, while the spatiotemporal behavior remains chaotic.

In the beginning of the simulation, 11 is replaced by 1011, which in turn is replaced by 10111001 and 1011100110011001. All these strategies give spatiotemporal chaos together with TFT. Tit-for-Tat is then itself replaced by the memory 3 strategy 01011101. Fig. 18c shows a configuration where 01011101 is in the process of invading. This strategy forms chaotic domains together with the memory 4 strategy 0011100110011001.

Fig. 18b shows how 1001 attempts to invade

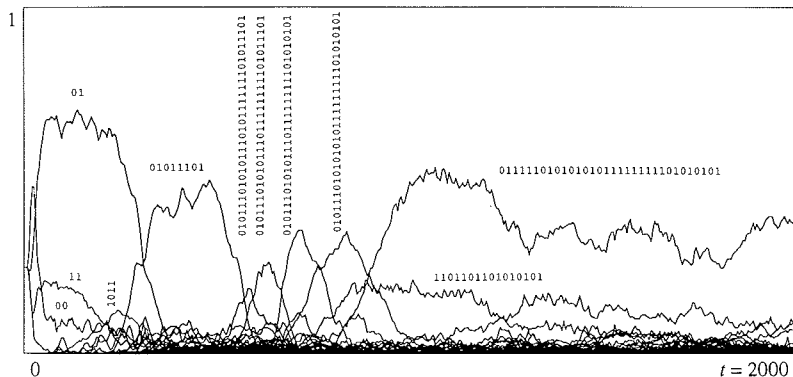


Fig. 17. Population densities as function of time for the parameter values  $(p, q) = (1.95, 0.95)$ ,  $p_{err} = 0.01$ . 2000 generations of the simulation are shown.

the chaotic state, which at that point consists of 01 and 1011. These attempts invariably fail—domains of 1001 can grow in the chaotic background, but internal mutations to 1000, 0001, or 00 create domains that spread with the speed of light inside the 1001 region. When these catch up with the more slowly expanding border of the 1001 domain, the chaotic state can reinvade and recapture the territory.

Fig. 18d shows an example of spatiotemporal chaos persisting at even longer memory. At these parameter values, we find rapid evolution towards larger complexity in the strategy space, while the spatial dynamics almost always can be characterized as spatiotemporal chaos.

Our final example has  $(p, q) = (1.8, 0.8)$ , and  $p_{\text{err}} = 0.01$  (region 6 in Fig. 13). Here we initially find irregular wave front activity (see Fig. 19a), but when memory 2 strategies enter spiral waves start appearing. One possible combination of species that gives spiral waves is 01, 0111 and 1101.

At first, we find a situation where spiral wave patches compete with other patches (see Fig. 19b). For shorter memory, the spiral waves are typically not very stable against mutations (and invasions). Longer memory strategies can form very stable spiral waves – the configuration shown in Fig. 19c is taken from a period of stasis where spiral waves containing the strategies

01011100, 0111101101011101, and  
 0111100101011001 dominate.

At the end of this simulation, the spiral waves have been replaced by a frozen state with a large diversity of patches of different strategies, see Fig. 19d. Mutations can trigger avalanches of activity that change the frozen state locally. This is an example of how the spatial degrees of freedom give the possibility of supporting a significantly higher degree of diversity than in the mean-field model.

## 7. Discussion

We have observed a number of phenomena in the spatial model that have no correspondence in the model where all pairwise interactions are included: coexistence through space-time chaos, formation of complex communities due to coexistence in different spatial regions, transitions between different forms of spatiotemporal behavior when parameters are varied, and also more open-ended evolutionary processes in some regions of the parameter space.

The model assumed a homogeneous environment. To observe other forms of spatial behavior related to the heterogeneity of the environment, it might be necessary to introduce explicit re-

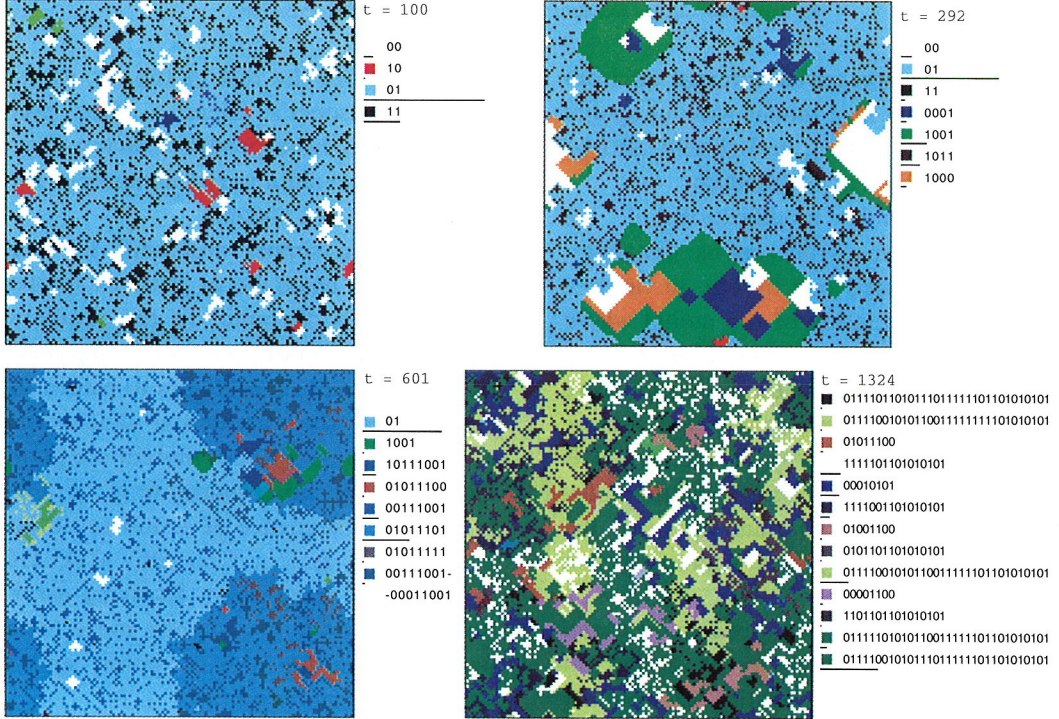


Fig. 18. Examples of lattice configurations during a simulation with  $(p, q) = (1.95, 0.95)$ ,  $p_{\text{err}} = 0.01$ : (a)  $t = 100$ ; (b)  $t = 291$ ; (c)  $t = 601$ ; (d)  $t = 1324$ .

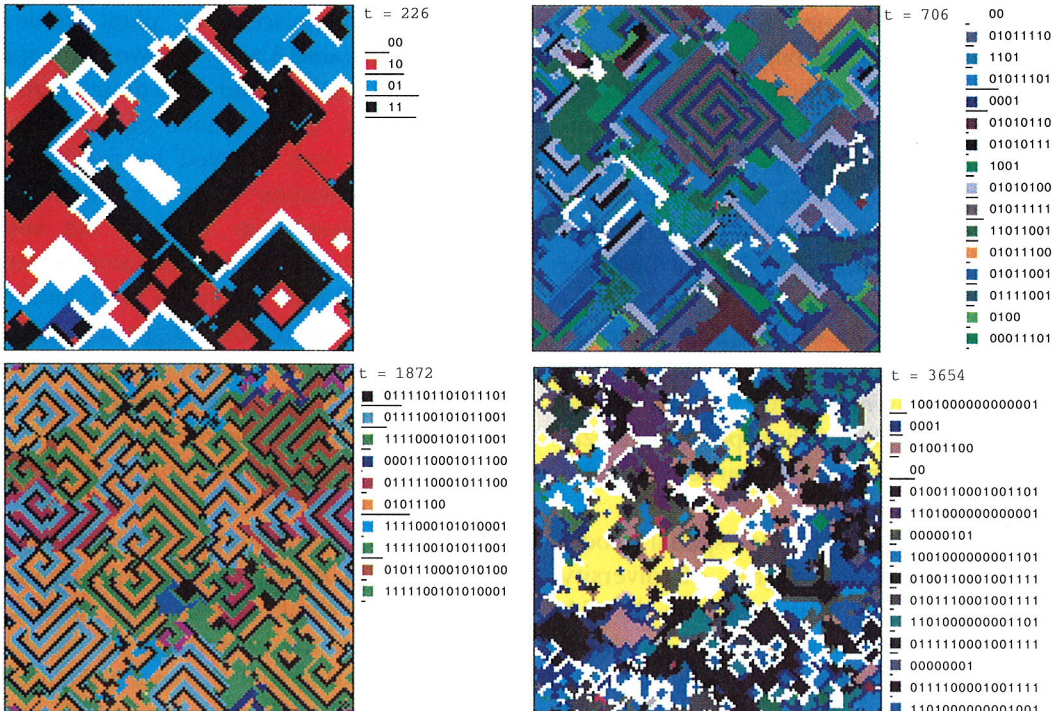


Fig. 19. Examples of lattice configurations during a simulation with  $(p, q) = (1.8, 0.8)$ : (a)  $t = 226$ ; (b)  $t = 706$ ; (c)  $t = 1872$ ; (d)  $t = 3654$ .

source flows and a non-trivial external environment. This was done in a model without spatial degrees of freedom in [10], and should also be done with spatial degrees of freedom.

Another conceivable modification of the model is to consider asynchronous dynamics, where sites are updated one by one in random order. In the interpretation of the model where sites represent individuals, one could argue that global synchronization is unnatural (though there certainly are biological contexts where a discrete time approach is appropriate). If the model is viewed as a coarse-grained discrete spatial model analogous to a partial differential equation, the synchronization issue becomes somewhat less important.

In Ref. [19] it was argued (apparently based on simulations for a single choice of the pay-off matrix) that asynchronous updating significantly changes the spatial dynamics of cooperators and defectors, and that coexistence does not occur in the asynchronous case.

We have repeated several of the simulations above with asynchronous updating instead of the CA dynamics. This results only in a few minor changes to the phase diagram of Fig. 13 (the microscopic phase diagram of Fig. 10 is unchanged). The chaotic region 2 does indeed disappear, as remarked for the related memory 0 case in [19], but the other chaotic region (region 7) still gives coexistence in a locally unstable system.

The small length scale of the spiral waves in region 5 makes it essentially impossible for them to organize in the asynchronous system. On the other hand, it seems likely that spatial organization could be found on much larger length scales in the asynchronous case.

In general, the asynchronous spatial model still supports the higher degree of diversity observed in many cases in the cases in the CA model, and in the same way as in the CA model we find several mechanisms for locally unstable but globally stable coexistence.

One could also consider other games, i.e.,

further explore the rest of the  $(p, q)$ -plane, not just the Prisoner's dilemma. Our preliminary investigations have produced many examples of interesting evolutionary dynamics for other games (such as Chicken).

There is a simple argument for why some other games could be at least as interesting as the Prisoner's dilemma. In the simulations, we see the evolution of error correcting mechanisms that allow a pair of strategies to return to mutual cooperation after accidental defections. If we follow the game in time, mutual cooperation is a fixed point. In other games (e.g.,  $p > 2$ ,  $q < 0$ ), the preferred sequence of action could be a cycle of period 2,  $(\dots, \text{CD}, \text{DC}, \text{CD}, \text{DC}, \dots)$ , rather than a fixed point. Evolving error correction for a 2-cycle is a slightly more complicated problem than for a fixed point, and requires somewhat longer memory.

One of the more interesting aspects of the spatial model is the possibility of generating communities with a high degree of diversity. Frozen patchy states such as that of Fig. 19d are somewhat reminiscent of plant communities. There are around  $3 \times 10^5$  known plant species on earth, which all depend on a quite small number of resources. The number of plant species is much larger than allowed by results based on ordinary population dynamics, which limit the number of species in terms of the number of resources [20,21]. Static explanations for this in terms of different equilibria in a heterogenous environment have been suggested (e.g., [22]). The existence of very diverse states in the spatial model suggest that the dynamics can generate diversity even in a homogenous spatial system.

Finally, we would like to emphasize the large variety of behavior found in the spatial model even inside the Prisoner's dilemma region. A label such as Prisoner's dilemma can sometimes lead one to think that a single unique model exists. For spatial or iterated games, this is not the case. The spatial Prisoner's dilemma really contains many different games, with widely different dynamics. One lesson to learn from this is

that conclusions about the evolution of cooperation based on the Prisoner's dilemma should not be trusted unless they are insensitive to variations in parameters such as the pay-off matrix.

## Acknowledgement

This research was supported by the Swedish Natural Science Research Council.

## References

- [1] R. Axelrod, *The evolution of cooperation* (Basic Books, New York, 1984).
- [2] E. Mayr, Change of genetic environment and evolution, in: *Evolution as a process*, J. Huxley, A.C. Hardy and E.B. Ford, eds. (Allen and Unwin, London, 1954) pp. 157–180.
- [3] E. Mayr, *Evolution and the diversity of life* (Harvard Univ. Press, Cambridge, MA, 1976).
- [4] N. Eldredge and S.J. Gould, Punctuated equilibria: an alternative to phyletic gradualism, in: *Models in Paleobiology*, T.J.M. Schopf, ed. (Freeman Cooper, San Francisco, 1972) pp. 82–115.
- [5] M.C. Boerlijst and P. Hogeweg, Spiral wave structure in prebiotic evolution: hypercycles stable against parasites, *Physica D* 48 (1991) 17–28.
- [6] M.C. Boerlijst and P. Hogeweg, Self-structuring and selection; spiral waves as a substrate for prebiotic evolution, in: *Artificial Life II*, C.G. Langton, J.D. Farmer, S. Rasmussen and C. Taylor, eds. (Addison-Wesley, Redwood City, CA, 1991) pp. 255–276.
- [7] M. Eigen and P. Schuster, *The hypercycle: A principle of natural self-organization* (Springer, Berlin, 1979).
- [8] M.P. Hassell, H.N. Comins and R.M. May, Spatial structure and chaos in insect population dynamics, *Nature* 353 (1991) 255–258.
- [9] K. Lindgren, Evolutionary phenomena in simple dynamics, in: *Artificial Life II*, C.G. Langton, J.D. Farmer, S. Rasmussen and C. Taylor, eds. (Addison-Wesley, Redwood City, CA, 1991) pp. 295–312.
- [10] K. Lindgren and M.G. Nordahl, Artificial food webs, in: *Artificial Life III*, C.G. Langton, ed. (Addison-Wesley, Reading, MA, 1993).
- [11] M.A. Nowak and R.M. May, Evolutionary games and spatial chaos, *Nature* 359 (1992) 826–829.
- [12] M.A. Nowak and R.M. May, The spatial dilemmas of evolution, *Int. J. of Bifurcation and Chaos* 3 (1993) 35–78.
- [13] K. Matsuo, Ecological characteristics of strategic groups in 'dilemmatic world', in: *Proc. IEEE Int. Conference on Systems and Cybernetics* (1985) pp. 1071–1075.
- [14] N. Adachi and K. Matsuo, Ecological dynamics of strategic species in Game World, *FUJITSU Sci. Tech. J.* 28 (1992) 543–558.
- [15] K. Lindgren and M.G. Nordahl, in preparation.
- [16] A. Rapoport and M. Guyer, A taxonomy of  $2 \times 2$  games, *General Systems* 11 (1966) 203–214.
- [17] S.A. Kauffman, Metabolic stability and epigenesis in randomly constructed genetic nets, *J. Theor. Biology* 22 (1969) 437–467.
- [18] N. Packard, Complexity of growing patterns in cellular automata, in: *Dynamical Systems and Cellular Automata*, J. Demongeot, E. Goles and M. Tchuente, eds. (Academic Press, New York, 1985).
- [19] B.A. Huberman and N.S. Glance, Evolutionary games and computer simulations, *Proc. Natl. Acad. Sci.* 90 (1993) 7716–7718.
- [20] R.H. MacArthur and R. Levins, Competition, habitat selection and character displacement in a patchy environment, *Proc. Natl. Acad. Sci. USA* 51 (1964) 1207–1210.
- [21] S.A. Levin, Community equilibria and stability, an extension of the competitive exclusion principle, *American Naturalist* 104 (1970) 413–423.
- [22] D. Tilman, *Resource competition and community structure* (Princeton Univ. Press, Princeton, NJ, 1982).

